Kinetics and Motility of the Eg5 Microtubule Motor

Andrew Lockhart and Robert A. Cross*

Molecular Motors Group, Marie Curie Research Institute, Oxted, Surrey, RH8 OTL, U.K.

Received September 28, 1995; Revised Manuscript Received December 18, 1995[⊗]

ABSTRACT: We have investigated the kinetic properties of the slow plus end directed microtubule (MT) motor Eg5. The recombinantly expressed fusion protein E437GST, containing residues 12−437 of Eg5 fused to the N-terminus of glutathione *S*-transferase (GST), is dimeric and motile, translocating MTs at an average speed of 0.063 (±0.01) μm s^{-1}. The kinetics of ATP turnover by E437GST were investigated using the fluorescent ATP analogue methylanthraniloyl-ATP (mantATP). In the absence of MTs, mantADP release from E437GST is slow (0.006 s^{-1} in 50 mM NaCl) and rate-limiting. MTs accelerate this kinetic step ~850-fold to a maximal rate of 4.94 s^{-1}. Under these conditions, the steady-state rate of mantATP turnover was 1.92 s^{-1}, indicating that MT-activated mantADP release accounts for at least 40% of the total cycle time of the motor and is probably rate-limiting. This step is around 10-fold slower in Eg5 than in kinesin, consistent with it limiting the rate of physical stepping in both Eg5 and kinesin. The dissociation constants of the motor in the presence of various nucleotides were determined using MT pelleting assays. ADP stabilizes the weakest bound state of the motor, while ATP, ATPγS, AMPPNP, and apyrase all induce a shift toward tighter binding states. Overall, the data indicate that Eg5 displays strong kinetic homologies with the two other well-characterized MT motors, kinesin and non claret disjunctional, suggesting that all kinesin superfamily motors may share the same basic mechanochemistry.

Eg5 is a kinesin-like microtubule (MT)[1] plus end directed motor discovered in *Xenopus laevis* egg extracts (LeGuellec et al., 1991). It is a member of the bimC subfamily of MT motors (Goodson et al., 1994) and localizes to the mitotic spindle where it is thought to be involved in spindle assembly (Sawin et al., 1992). The motor is predicted from its primary sequence to have a three-domain structure: an N-terminal motor domain followed by a region of α-helix stalk, which is believed to form a coiled-coil, and a nonhelical C-terminal tail region (LeGuellec et al., 1991). The C-terminal tail domain contains a ~40 residue sequence, "the bimC box", which is partially conserved across most of the bimC family and is a potential target for a number of kinases (Heck et al., 1993). Recent work suggests that phosphorylation of Eg5 within the bimC box may control its localization to the spindle (Sawin & Mitchison, 1995).

Despite the fact that a large number of MT motor proteins have been identified, to date only two of these motors, kinesin and non claret disjunctional (ncd), have been kinetically characterized in any detail. Kinesin and ncd move in opposite directions, kinesin toward the plus ends (Vale et al., 1985) and ncd toward the minus ends of MTs (Walker et al., 1990). Although the mechanism of directional reversal is unknown, the available data suggest that these two oppositely-directed superfamily members share very similar kinetic characteristics. For both kinesin and ncd, a key feature of the mechanism is that ADP release is rate-limiting in the absence of MTs and is greatly accelerated by MT binding (Hackney, 1988; Gilbert et al., 1995; Lockhart et al., 1995a; Ma & Taylor, 1995a; Shimizu et al., 1995). Additionally, it is clear that the ADP states of the motors are weakly bound to MTs, while the nucleotide-free states which follow ADP release are strongly bound (Ma & Taylor, 1995; Crevel et al., 1996), suggesting that ADP release corresponds to a weak-to-strong transition.

Work from two different groups indicates that ADP release (corresponding to the weak-to-strong transition of an attached head) is the rate-limiting step of ncd's MT-activated ATPase (Lockhart et al., 1995a; Shimizu et al., 1995). For kinesin, there is currently some dispute over which step is rate-limiting at high microtubule concentrations. Gilbert et al. (1995) proposed that the dissociation of kinesin from MTs after ATP hydrolysis was rate-limiting. However, earlier work (Hackney, 1988; Gilbert & Johnston, 1994) and two other more recent studies (Lockhart et al., 1995a; Ma & Taylor, 1995a) indicate that ADP release is probably rate-limiting. This and the more general question of which kinetic steps determine the rate of physical stepping can be examined by studying a motor which moves at a markedly different rate to kinesin. Eg5 moves ~10−20-fold more slowly than kinesin, but in the same direction. A kinetic study of Eg5 amounts to a natural mutagenesis experiment, in which kinesin has been mutated to move slower, such that we can ask how the kinetic coupling of the slower "mutant" differs from the faster "wild type" kinesin. In this study, we show that Eg5 shows the same broad pattern of coupling (ADP induces weak binding, ATP analogues induce strong binding) and the same rate-limiting step (MT-activated ADP release) as kinesin and ncd. For all three enzymes, the physical transition coupled to ADP release corresponds to a switch from weak to strong MT binding. This step is around 10-fold slower in Eg5 than in kinesin, consistent with it limiting the rate of physical stepping in both kinesin and Eg5.

* Corresponding author. Phone: (0)1883 722306. Fax: (0)1883 714375. E-mail: Rob@biomotor.demon.co.uk.

[⊗] Abstract published in *Advance ACS Abstracts,* February 1, 1996.

[1] Abbreviations: AMPPNP, 5′-adenylylimidodiphosphate; ATPγS, adenosine 5′-*O*-(3-thiotriphosphate); DTT, dithiothreitol; GST, glutathione *S*-transferase; mantATP, methylanthraniloyl-ATP; MTs, microtubules; ncd, non claret disjunctional; PCR, polymerase chain reaction; PIPES, piperazine-*N*,*N*′-bis(2-ethanesulfonic acid); SDS−PAGE, sodium dodecyl sulfate−polyacrylamide gel electrophoresis.

0006-2960/96/0435-2365$12.00/0

EXPERIMENTAL PROCEDURES

Materials. Restriction enzymes, Vent DNA polymerase, and DNA-modifying enzymes were obtained from New England Biolabs (Hitchin, U.K.). ATPγS and complete protease inhibitor cocktail tablets were obtained from Boehringer Mannheim (Lewes, U.K.). *N*-Methylisatoic anhydride was obtained from Cambridge Bioscience (Cambridge, U.K.). The pET17b vector was obtained from AMS Biotech. Ltd. (Oxon, U.K.). Chromatography materials were purchased from Pharmacia Biotech (St. Albans, U.K.). All other chemicals were obtained from Sigma (Poole, U.K.). The RETRAC tracking software package was obtained from the Institute of Applied Biology, University of York (E-mail: NJC1@york.ac.uk).

Construction of E437GST. All constructs were produced using the Eg5K2 gene which is 93% identical to the original Eg5 cDNA clone and is probably a consequence of pseudotetraploidy in *Xenopus laevis* (LeGuellec et al., 1991). Neither of the constructs encode the N-terminal amino acids MSSQNSFMSSKK, although previous work has demonstrated that these amino acids are not required for *in vitro* motility (Sawin et al., 1992) or localization of the motor to the spindle (Sawin & Mitchison, 1995). In addition, it is unclear which of the methionines represents the translational start, and accordingly, all constructs are numbered assuming that the first methionine of the Eg5K2 clone represents the translational start.

E437GST, encoding residues 12−437 of Eg5 fused to the N-terminus of glutathione *S*-transferase (GST), was constructed by amplifying an ∼1300 bp fragment from the Eg5K2 clone using 5′-GATATACATATGGCCAGCAAGAAGGAGGAC-3′ and 5′-GTA**CTA**GTTGAATTCACTGATGCTCTTCAGTTCCTCCTCCATGGCAG-3′ as the forward and reverse primers, respectively, the forward primer introducing an *Nde*I site (underlined) onto the 5′-end of the DNA and the reverse primer introducing an *Spe*I site [containing an in-frame stop codon (boldface)] and an *Eco*RI site. PCR reactions were performed using the proofreading thermostable DNA polymerase Vent and used 20 cycles of amplification to minimize the chance of random errors in the PCR-generated gene. The amplified DNA was purified from an agarose gel, digested with *Nde*I/*Spe*I, and ligated into *Nde*I/*Spe*I-cut pET17b. This plasmid termed pETE437 was digested with *Eco*RI and ligated to a 660 bp DNA fragment encoding the GST gene with *Eco*RI sticky ends and an in-frame stop codon at its 3′-end to create the plasmid pETE437GST.

Expression and Purification of E437GST. Expressions were performed in BL21(DE3) cells freshly transformed with the pETE437GST plasmid. Overnight cultures of bacteria were diluted 1 in 50 into 2×YT medium supplemented with ampicillin (50 μg/mL) and grown, with shaking, at 37 °C until the absorbance at 600 nm was 1.0. The cells were shaken for a further 30 min at 30 °C before induction with isopropyl β-D-thiogalactopyranoside (0.4 mM), and after a further 4 h shaking at 30 °C, the bacteria were harvested by centrifugation. The cell pellets were frozen in liquid nitrogen and stored at −80 °C.

Cell pellets were resuspended in buffer A (20 mM PIPES, pH 6.9, 1 mM DTT, and 5 mM $MgCl_2$), supplemented with complete protease inhibitor cocktail tablets at the recommended dosage and incubated on ice with lysozyme (0.1 mg/mL) for 20 min. The cell lysate was supplemented with Triton X-100 (0.05%) and deoxyribonuclease I (40 μg/mL) and incubated for a further 10 min on ice. The supernatant was clarified by centrifugation (27000*g*, 50 min, 4 °C) and the cell pellet discarded. All chromatography steps were performed using an FPLC system (Pharmacia Biotech, St. Albans, U.K.) at 4 °C. E437GST was purified by passing the clarified supernatant over a 10 mL glutathione−Sepharose 4B column equilibrated in buffer A. After extensive washing of the column with buffer A, bound protein was eluted with buffer A supplemented with 20 mM reduced glutathione and 50 mM NaCl. The eluted fusion protein was then applied to a 1 mL Mono SP column equilibrated in buffer A plus 50 mM NaCl. E437GST was step-eluted from the column using buffer A supplemented with 300 mM NaCl. Column fractions were analyzed for purity by SDS−PAGE (Laemmli, 1970) and the peak fractions pooled. Frozen protein stocks were prepared by supplementing the purified protein solution with 10% glycerol, flash-freezing aliquots in liquid nitrogen, and storing at −70 °C. When stored in this manner, the protein was stable for at least 2 months and once thawed was used immediately.

Expression and Purification of E437. Expressions were performed in BL21(DE3) cells freshly transformed with the pETE437 plasmid using the same method as described for E437GST. Cells containing E437 were resuspended in buffer A and lysed as described above. The clarified supernatant was passed over a 5 mL Mono SP column equilibrated in buffer A. E437 was eluted from the column using buffer A supplemented with 300 mM NaCl. The peak fractions containing E437 were frozen in liquid nitrogen and stored at −70 °C.

Calculation of Protein Concentration. Protein concentrations were estimated spectrophotometrically based on extinction coefficients calculated from the protein's primary sequence, using values of 5690 M^{-1} cm^{-1} and 1280 M^{-1} cm^{-1} for the extinction coefficients of tryptophan and tyrosine at 280 nm, respectively (Gilbert & Johnson, 1993). As the protein was purified with bound ADP, an extra extinction coefficient of 2500 M^{-1} cm^{-1} per ADP was added to the calculated extinction coefficients (Gilbert & Johnson, 1993) to give a value of 69 700 M^{-1} cm^{-1} for E437GST. The concentration of E437GST in all experiments is expressed per single polypeptide chain (i.e., per motor domain).

Estimation of Stokes Radii. The Stokes radii (R_s) of E437GST and E437 were determined using a Superose 12 gel filtration column equilibrated in 20 mM PIPES, pH 6.9, 1 mM DTT, 5 mM $MgCl_2$, and 100 mM NaCl. The column was calibrated with proteins of known R_s: bovine pancreas ribonuclease A (1.64 nm), bovine pancreas chymotrypsinogen A (2.09 nm), hen egg ovalbumin (3.05 nm), bovine serum albumin (3.55 nm), and yeast alcohol dehydrogenase (4.6 nm).

Estimation of Sedimentation Coefficients. Sedimentation coefficients ($s_{20,w}$) were determined by rate zonal centrifugation on a 15%−30% glycerol gradient in 20 mM PIPES, pH 6.9, 1 mM DTT, 5 mM $MgCl_2$, and 100 mM NaCl. The gradients were centrifuged at 50 000 rpm in a TST60.4 rotor (Sorvall) for between 20 and 24 h. Bovine serum albumin (4.6 S), rabbit muscle creatine kinase (5.3 S), rabbit muscle aldolase (7.3 S), and bovine liver catalase (11.3 S) were run as standards. Plots of the relative distances travelled by the standards versus their sedimentation coefficients yielded

straight lines from which the sedimentation coefficients of both proteins were estimated.

Estimation of Molecular Masses. The molecular masses of E437GST and E437 were calculated by cosedimenting E437GST with proteins of known molecular mass [rabbit muscle aldolase (150 kDa), rabbit muscle creatine kinase (82 kDa), bovine serum albumin (67 kDa), bovine pancreas chymotrypsinogen A (25 kDa), and bovine pancreas ribonuclease A (13.7 kDa)]. Rate zonal centrifugation was performed using a 15%−30% glycerol gradient in 20 mM PIPES pH 6.9, 1 mM DTT, 5 mM $MgCl_2$, and 100 mM NaCl. The gradients were centrifuged at 50 000 rpm in a TST60.4 rotor (Sorvall) for between 20 and 24 h. Plots of the relative distance travelled by the standards versus their log molecular masses yielded a straight line from which the molecular masses of E437GST and E437 were estimated according to the method of Freifelder (1982).

Purification and Polymerization of Tubulin. Tubulin was purified from porcine brain as described in Lockhart and Cross (1994). Tubulin (typically 5 mg/mL in 50 mM PIPES, pH 6.9, 1 mM EGTA, 0.2 mM $MgCl_2$, 0.01 mM GTP, and 20% glycerol) was polymerized by the addition of $MgCl_2$ and GTP to final concentrations of 2 mM and 1 mM, respectively. The tubulin was incubated for 30 min at 37 °C, at which point taxol was added to a final concentration of 10 μM. In order to remove guanine nucleotides, the taxol-stabilized MTs were pelleted by centrifugation (100000*g*, 10 min, 25 °C). The supernatant was removed and the MT pellet carefully resuspended in buffer A supplemented with taxol (10 μM). All MT concentrations are expressed per tubulin heterodimer.

MantATP Turnovers. MantATP was synthesized as described by Hiratsuka (1983) and purified on a DEAE-cellulose column developed with a linear 0.1−1 M triethylamine (pH 7.5) gradient. MantATP turnovers were performed in buffer A at 20 °C as described in Lockhart and Cross (1994).

Measurement of Steady-State MT-Activated ATPase Rates. Steady-state MT-activated ATPase rates were measured using a pyruvate kinase/lactate dehydrogenase-linked assay in buffer A supplemented with 10 μM taxol at 20 °C as described in Lockhart and Cross (1994). The amount of motor used in the assays was 0.2 μM of E437GST motor domains. The kinetic parameters k_{cat} and $K_{50\%,MT}$ (the concentration of MTs required for half-maximal activation) were obtained by least-squares fitting the MT activation data to rectangular hyperbolae using Kaleidagraph 3.0 (Synergy Software).

Measurement of MT-Activated Rates of MantADP Release. Stopped-flow experiments were performed using a Hi-Tech SF-61MX spectrofluorometer (Hi-Tech Scientific Ltd., Salisbury, U.K.) in the fluorescence mode using a path length of 1.5 mm. An excitation wavelength of 350 nm was used and the fluorescence observed using a filter with a cutoff wavelength of 375 nm; 1 mL drive syringes were used, resulting in a 2-fold dilution of the solutions after mixing. All experiments were performed in buffer A supplemented with 10 μM taxol at 20 °C. E437GST (1 μM) was mixed with a 4-fold excess of mantATP. After 20 min, the fluorescent motor·mantADP complexes were rapidly mixed in the stopped-flow with MTs plus 2 mM Mg-ATP. Data from at least three injections were collected and averaged for each MT concentration.

Steady-State Measurements of MantATP Turnover. The turnover of mantATP by E437GST was monitored using a discontinuous malachite green assay to detect the production of inorganic phosphate (Itaya & Ui, 1966). Assays were performed in buffer A supplemented with 2 mM mantATP and 10 μM taxol at 20 °C.

Pelleting Assays Performed with a Fixed Concentration of MTs. Pelleting assays were performed in buffer A supplemented with taxol (10 μM) at 20 °C. E437GST (0.25, 0.5, 1, 2, 4, 6, 8, and 10 μM) was added to taxol-stabilized MTs (2.5 μM) in the presence of either ATPγS (4 mM), AMPPNP (2 mM), ATP (5 mM), ADP (2 mM), or apyrase (0.1 milliunit; grade VII, Sigma) in a volume of 40 μL. The final concentration of NaCl in the assays was 60 mM. The samples were gently mixed and centrifuged in a Beckman TLX100 ultracentrifuge (100000*g*, 10 min, 20 °C). The supernatants were carefully removed, supplemented with 20 μL of SDS−gel loading buffer, and boiled for 5 min. The pellets were resuspended in 60 μL of SDS−gel loading buffer and boiled for 5 min. Equal amounts of pellet and supernatant were analyzed by SDS−PAGE on a 12.5% polyacrylamide microslab gel (Laemmli, 1970). After electrophoresis, the gels were stained with Coomassie Brilliant Blue R-250 to visualize the protein bands for analysis.

Grayscale CCD video images of the stained gels were captured into a Macintosh computer using a Scion AG-5 framegrabber and the relative integrated intensities of the protein bands in the supernatants and pellets determined using NIH Image 1.55 (Freeware). The amount of sample loaded on the gels was optimized to ensure a linear relationship between the amount of protein loaded and the integrated stain density. Dissociation constants and binding stoichiometries (expressed as the number of E437GST motor domains per tubulin heterodimer) were obtained by fitting rectangular hyperbolae to plots of the concentration of motor in the pellet versus its concentration in the supernatant using Kaleidagraph 3.0. Values for the binding stoichiometries were corrected for the small amount (∼2.5%) of MTs which did not pellet during the assays.

Pelleting Assays Performed with a Fixed Concentration of E437GST. Pelleting assays were performed in buffer A supplemented with taxol (10 μM) at 20 °C. A fixed concentration of motor (1 μM of E437GST motor domains) was titrated against increasing concentrations of taxol-stabilized MTs (1.25, 2.5, 5, 10, 15, 20, and 25 μM) in the presence of either ATP (5 mM), ADP (2 mM), or AMPPNP (2 mM). The assays were performed in a volume of 40 μL, and the final concentration of NaCl was 10 mM. The samples were gently mixed before centrifuging in a Beckman TLX100 ultracentrifuge (100000*g*, 10 min, 20 °C). The supernatants were carefully removed, and 20 μl of SDS−gel loading buffer was added. The pellets were resuspended in 30 μL of SDS−gel loading buffer. Equal amounts of pellet and supernatant were analyzed by SDS−PAGE on a 12.5% polyacrylamide microslab gel (Laemmli, 1970). After electrophoresis, the gels were stained with Coomassie Brilliant Blue R-250 to visualize the protein bands. The gels were analyzed as described above in order to quantitate the amount of E437GST in the MT pellet. Plots of the fractional binding of the motor versus MT concentration were fitted to rectangular hyperbolae to determine binding affinites and the maximal binding of the motor.

Table 1: Physical Properties of E437GST and E437[a]

	R_s (nm)	$s_{w,20}$ (S)	calcd molecular mass (kDa)	polypeptide molecular mass (kDa)	association state
E437GST	6.6, 5.1	6.3	127.0	74.0	dimer
E437	3.4	5.9	98.7	48.4	dimer

[a] Stokes radii (R_s) were determined by gel filtration chromatography and the sedimentation coefficients ($s_{w,20}$) by rate zonal centrifugation. The calculated molecular mass was determined according to Freifelder (1982) and the polypeptide molecular mass from the protein's primary sequence.

In Vitro Motility Assays. Motility assays were performed by binding the purified E437GST directly to a glass coverslip sealed to a microscope slide with grease to form a flow cell. The flow cell was then perfused with motility assay buffer [BRB 80 buffer (80 mM PIPES, pH 6.9, 1 mM $MgCl_2$, and 1 mM EGTA) supplemented with 10 μM taxol, 1 mM DTT and 1 mM Mg-ATP] and then with taxol-stabilized MTs (4 μM) resuspended in motility buffer. Microtubule movement was observed using video-enhanced differential interference contrast microscopy. The rate of MT movement was measured from the video images using the commercial tracking software package RETRAC.

RESULTS

Physical Characterization of E437GST. E437GST could be efficiently expressed in *E.* coli over a range of temperatures from 22 °C to 37 °C, although the optimal temperature for the expression of soluble protein was found to be at 30 °C. Rapid purification of the protein was facilitated by the use of glutathione affinity chromatography followed by ion-exchange chromatography on S-Sepharose and was easily completed in 1 day. Typical yields of E437GST were ~0.5 mg of protein per liter of bacterial culture.

The results of the rate zonal centrifugation are consistent with E437GST forming stable dimers in solution (Table 1). Although behaving as a single species during the rate zonal centrifugation, E437GST resolved into two peaks (of approximately equal area) during gel filtration chromatography (Table 1). A similar pattern of behavior was reported previously for the ncd−GST fusion protein GST−MC5, and the two peaks observed during gel filtration were attributed to the protein forming a mix of dimers and tetramers (Chandra et al., 1993). It is possible, however, that, in one or both cases, the two species resolved in the gel filtration may simply represent two different conformations of the "dumb-bell" shaped fusion proteins (which are basically two globular domains separated by a stalk region): a compact "folded" form and a more elongated "open" form of the protein. Both native myosin and native kinesin show a similar conformational flexibility which is associated with controlling the motors' activity (Hackney, 1992). In the case of GST−MC5, proteolytic removal of the GST tag resulted in stable, dimeric motor, MC5, whose kinetic behavior was similar to that of the uncleaved fusion protein (Lockhart & Cross, 1994).

The influence of the GST moiety on the association state of E437GST was therefore investigated by expressing the motor without the GST tag. Gel filtration experiments indicate that E437 elutes as a single peak, and the results from rate zonal centrifugation are consistent with the motor forming stable dimers in solution (Table 1). These data demonstrate that GST does not influence the dimerization of E437GST. One effect, however, resulting from the removal of GST was that the amount of soluble motor recovered from the bacteria was significantly reduced making E437 unsuitable for detailed kinetic analysis.

The ability of E437GST to translocate MTs in *in vitro* motility assays was also investigated. The motor was found to move MTs at an average velocity of ~0.063 (±0.01) μm s^{-1}, which is around twice as fast as originally reported for Eg5 (Sawin et al., 1992) and may be due to the different location of the GST in the two studies (see Discussion). Another difference between this and the earlier study is that smooth movement of MTs by the motor occurred at 1 mM Mg-ATP, whereas the construct used in the original study required 10 mM (Sawin et al., 1992).

Rate-Limiting ADP Release in the Absence of MTs. The turnover of ATP by E437GST was investigated using the fluorescent ATP analogue methylanthraniloyl-ATP (mantATP). A slow enhancement in the fluorescence of mantATP was obtained when the analogue was incubated with E437GST and represents the binding of the mantATP into the active site of the motor (Figure 1a). The mantATP is efficiently hydrolyzed by the motor at a rate of ~0.01 s^{-1} (in buffer supplemented with 50 mM NaCl, 20 °C). The steady-state level of the fluorescent enhancement remains stable, indicating that the product, mantADP, is essentially trapped by the motor. Addition of a large excess of Mg-ATP results in a slow decrease in fluorescence to its base line level as the ATP exchanges with the mantADP at the motor's active site (Figure 1b). The transients for both these reactions fit to single exponentials to give rates for mantATP binding and mantADP loss from the motor. At low ionic strength (50 mM NaCl), the rates of mantATP binding and mantADP release were 0.008 and 0.006 s^{-1}, respectively. Both rates showed marked increases at higher ionic strengths, with the rate of mantATP binding to the motor almost doubling and the mantADP release rate increasing 4-fold between 50 and 200 mM NaCl (Figure 1c). A similar ionic strength dependence has been observed for ncd (Lockhart & Cross, 1994).

Increasing the concentration of mantATP used in the reactions (up to 10-fold) produced no significant increase in the rate of mantATP binding to the motor. Taken together with the similarity in the rates of mantATP binding and mantADP loss from the motor, these results indicate that, like ncd (Lockhart & Cross, 1994; Shimizu et al., 1995) and kinesin (Hackney, 1988; Gilbert & Johnson, 1993; Ma & Taylor, 1995b), Eg5 copurifies with ADP in its active site. Thus, the rate of mantATP binding is limited by the loss of the prebound ADP from the motor.

Attempts to examine nucleotide binding to nucleotide-free Eg5 have so far been unsuccessful. Treatment of mant-labeled motor with 10−50 mM EDTA strips the nucleotide from the motor. However, after addition of excess Mg^{2+} to the stripped motor and mixing with excess mantATP, only a slow rebinding of the nucleotide is observed, consistent with the stripping conditions partially denaturing the motor. Similar findings have been reported when attempting to strip ncd of its tightly bound ADP (our published observations; Shimizu et al., 1995).

MT-Activated ATPase. The ability of MTs to activate the ATPase of E437GST was investigated using a steady-state-

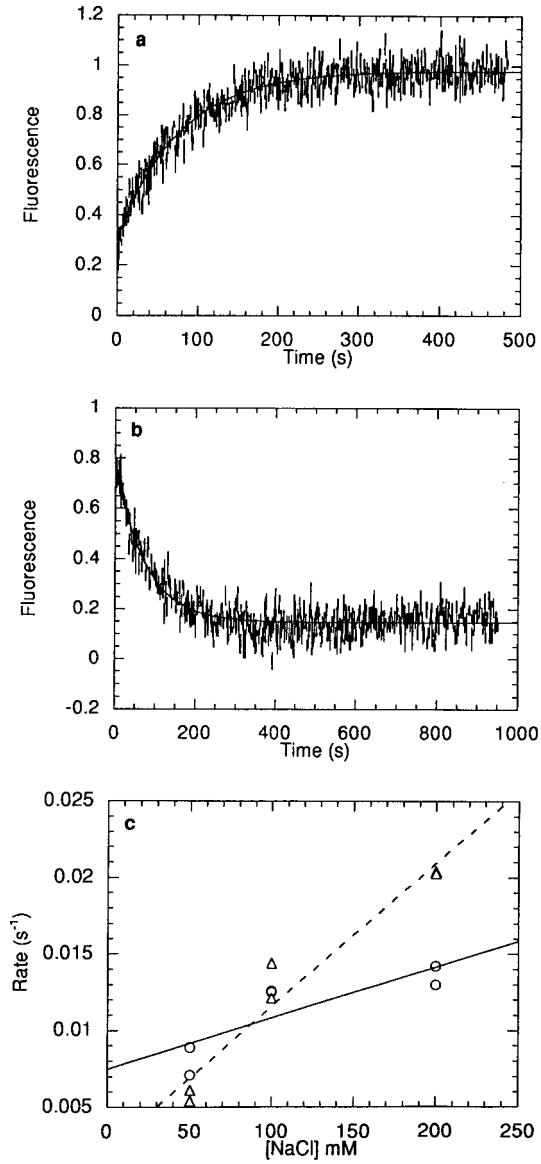

FIGURE 1: Time course showing the turnover of mantATP by E437GST. (a) Incubation of mantATP (5 μM) with E437GST (4 μM) in buffer A supplemented with 50 mM NaCl. (b) After completion of the binding reaction, Mg-ATP (1.32 mM) was added as a chase. The data in both panels were fitted to single exponentials, represented by the smooth lines, to give rates for mantATP binding and mantADP release of 0.008 and 0.006 s^{-1}, respectively. (c) Dependence of mantATP binding (○) and mantADP release (△) rates on NaCl concentration.

linked assay which detects the production of ADP by the motor (Figure 2). ATP turnover by E437GST is strongly accelerated by MTs to a k_{cat} of 1.42 (±0.13) s^{-1} at low ionic strength (25 mM NaCl). The amount of MTs required for half-maximal activation ($K_{50\%,MTs}$) was 0.37 (±0.12) μM, and the K_m for ATP (at 1 μM MTs) was 13 (±2.5) μM.

The effect of ionic strength on MT-activated ATP turnover by E437GST was also investigated by performing the assays in the presence of 100 mM NaCl. The k_{cat} and $K_{50\%,MTs}$ values under these conditions were 0.58 (±0.03) s^{-1} and 0.25 (±0.06) μM, respectively (Figure 2). The decrease in the k_{cat} value with increasing ionic strength is consistent with the findings of other studies on both ncd (Lockhart & Cross, 1994; Shimizu et al., 1995) and kinesin (Ma & Taylor, 1995a). However, the slight decrease in the $K_{50\%,MTs}$ value, as the ionic strength of the buffer increased, is in sharp

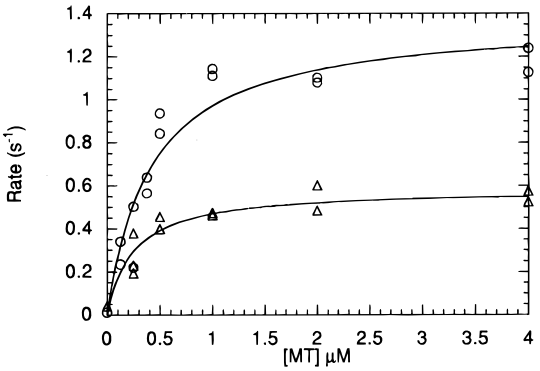

FIGURE 2: Steady-state measurements of the MT activation of ATP turnover by E437GST at 25 mM NaCl (○) and 100 mM NaCl (△). The ATPase activity is expressed per E437GST motor domain and the MT concentration expressed per tubulin heterodimer. The data were fitted to rectangular hyperbolae to derive values for the kinetic constants k_{cat} and $K_{50\%,MTs}$.

contrast to the significant increases in this value found with both kinesin (around 8-fold; Ma & Taylor, 1995a) and ncd (around 10-fold; Lockhart & Cross, 1994).

MT-Activated MantADP Release. The MT-activated rates of mantADP release from E437GST were measured by mixing fluorescent motor·mantADP complexes with MTs in the presence of 1 mM Mg-ATP (to stop any rebinding of the mant nucleotide) in a stopped-flow spectrofluorometer. The rates of mantADP release were obtained by fitting the stopped-flow traces to two exponentials (Figure 3a). The slow phase of the exponential was ignored as it was independent of MT concentration, represented between only 10 and 20% of the total amplitude, and was much slower than the rate of mantATP turnover under these conditions. MTs were found to stimulate mantADP release from E437GST to a maximum rate of 4.94 (±0.21) s^{-1} (Figure 3b). The concentration of MTs required for the half-maximal rate ($K_{50\%,\ mADP}$) was 1.28 (±0.23) μM. The MT-activated steady-state turnover of mantATP by E437GST was similar to that of authentic Mg-ATP with k_{cat} and $K_{50\%,MTs}$ values of 1.94 (±0.07) s^{-1} and 0.53 (±0.07) μM, respectively (Figure 3c).

Assuming a cycle time of ~500 ms, these data indicate that the motor spends at least 200 ms (or ~40% of the total cycle time) in the ADP state. Considering that there must be at least three steps (ATP binding, ATP hydrolysis, and phosphate release) prior to ADP release, it is highly unlikely that there is another comparably slow step. This indicates that MT-activated mantADP release is probably rate-limiting for Eg5.

Comparison of the MT dependence for mantADP release and steady-state mantATP hydrolysis indicates that the $K_{50\%,mADP}$ is almost 2-fold greater than the $K_{50\%,MTs}$, suggesting that other factors, including the possibility that Eg5, like kinesin (Hackney, 1995), is processive, contribute to the steady-state cycling of E437GST.

Pelleting Assays Performed with a Fixed Concentration of MTs. MT pelleting assays were used to investigate the binding affinities and binding stoichiometries of E437GST in the presence of different nucleotides (ATP, ADP) and nucleotide analogues (AMPPNP, ATPγS). The enzyme apyrase (which scavenges and hydrolyzes ATP and ADP to AMP) was also added to the assays in order to generate a nucleotide-free form of the motor. The resulting pellets and

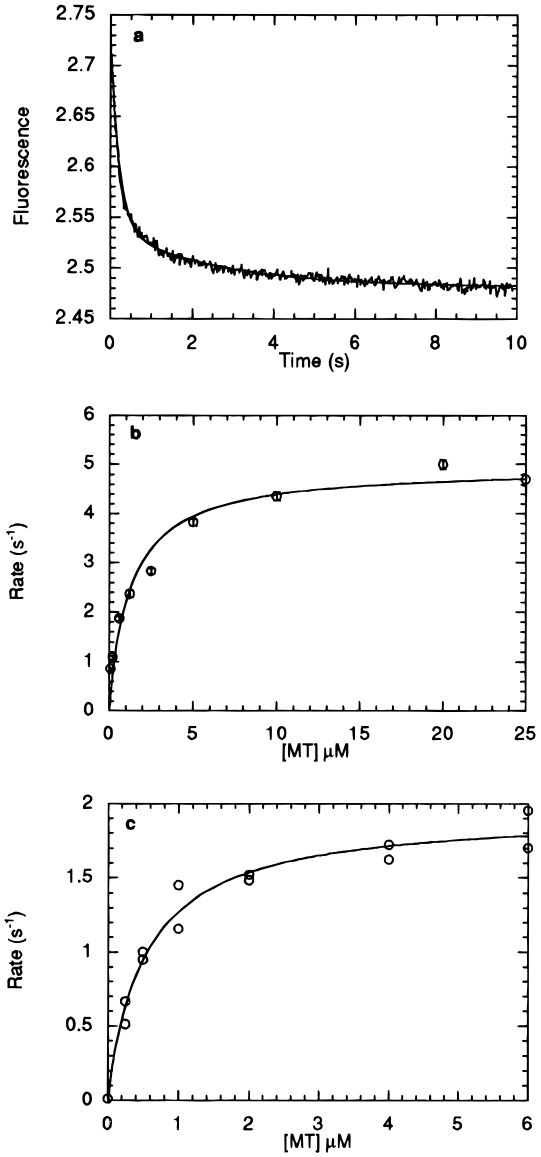

FIGURE 3: MT-activated rates of mantADP release from E437GST. (a) Representative stopped-flow trace for E437GST (0.5 μM) labeled with mantADP (2 μM) and rapidly mixed with MTs (25 μM) plus Mg-ATP (1 mM). Concentrations are those in the flow cell after mixing. The solid black curve is the best fit of the data to two exponentials and gives a mant ADP release rate of 4.69 s^{-1}. (b) MT dependence of mantADP release rates from E437GST. Each data point is the average of at least three separate stopped-flow traces. The solid black line is the best fit of the data to a rectangular hyperbola to give an estimated maximal rate of 4.94 s^{-1} and a half-maximal rate at 1.28 μM. (c) Steady-state measurement of MT-activated mantATPase of E437GST. The ATPase activity is expressed per E437GST motor domain and the MT concentration expressed per tubulin heterodimer. The data were fitted to a rectangular hyperbola to give a k_{cat} of 1.94 s^{-1} and a half-maximal rate at 0.53 μM.

supernatants were analyzed by SDS−PAGE and are shown in Figure 4. The binding isotherms for E437GST are shown in Figure 5 with the dissociation constants (K_d's) and binding stoichiometries summarized in Table 2. In the absence of added nucleotide, the binding of E437GST is relatively tight (K_d = 2.22 μM). Addition of Mg-ADP to the assay results in a large decrease in the affinity of the motor for the MTs, which although we were unable to quantitate due to the weakness of the interaction, is estimated to be in excess of 10 μM under these conditions. Mg-ATP also greatly reduced the binding affinity of the motor, and again we estimate a K_d > 10 μM, consistent with the motor·ADP state predominating under steady-state conditions.

By contrast, the binding of E437GST in the presence of the nonhydrolyzable analogue AMPPNP and the slowly hydrolyzable analogue ATPγS both result in an increase in the affinity of the motor for the MTs, with K_d's of 0.02 and 7.74 μM, respectively. In both cases, it is unclear which state(s) the analogues mimic during the ATPase cycle. This is especially true of AMPPNP, which binds extremely weakly to both kinesin and ncd (Crevel et al., 1996). The results obtained with ATPγS, however, do suggest that either the ATP or the ADP·P$_i$ states bind with higher affinity than the ADP state. Treatment of E437GST with apyrase to generate a nucleotide-free form of the motor produced a 2-fold increase in the affinity of the motor compared to the no added nucleotide state and results in a K_d of 1.06 μM. With the exception of AMPPNP, this is the most tightly bound state of the motor.

In apyrase and with no added nucleotide, the binding of the motor saturated at two E437GST motor domains (i.e., one E437GST dimer) per tubulin heterodimer. ATPγS also produced a good fit to this binding stoichiometry, but the binding of the motor was so weak in the presence of ATP or ADP that no estimates could be made under these conditions. The binding isotherm obtained in AMPPNP produced a more complicated behavior than the other conditions (Figure 5c). The binding of E437GST appears to saturate at a binding stoichiometry of one motor domain per tubulin heterodimer, after which there is a weaker, possibly nonspecific, binding of the motor to the MTs. Given that there is no sign of nonspecific binding in the other nucleotides, this affect appears genuine. One interesting possibility is that under these conditions AMPPNP recruits an otherwise unstable conformation in which a single dimer can bridge two MT binding sites (on different heterodimers). Signs of a similar behavior were recently reported for kinesin in the presence of AMPPNP (Crevel et al., 1996), although earlier studies have reported stoichiometries consistent with only one head of dimer binding (Huang et al., 1994; Lockhart et al., 1995b).

Using an engineered single-headed form of Eg5 (residues 12−408), we have found the binding of this protein saturates at one motor domain per tubulin heterodimer, indicating that, as with kinesin (Harrison et al., 1993; Huang et al., 1994; Lockhart et al., 1995b), and ncd (Lockhart & Cross, 1994; Lockhart et al., 1995b) there is only one motor−head binding site per tubulin heterodimer. The current data are consistent with Eg5 negotiating the MT lattice in ~8 nm steps (the interdimer spacing of tubulin) utilizing a "head over head" mechanism as originally proposed for kinesin [for a review, see Block (1994)]. However, the two-heads-bound (bridge) structure (which must at least occur transiently during walking) may be kinetically more accessible for Eg5 than for ncd or kinesin.

Pelleting Assays Performed with a Fixed Concentration of E437GST. The binding of E437GST to MTs was also titrated by mixing a fixed amount of motor (1 μM) with increasing amounts of MTs. Under these conditions, the ratio of motor to MTs is considerably lower than in the pelleting assays described above and more akin to the conditions used in the steady-state ATPase assays. The assays were first performed in 2 mM AMPPNP and resulted in greater than

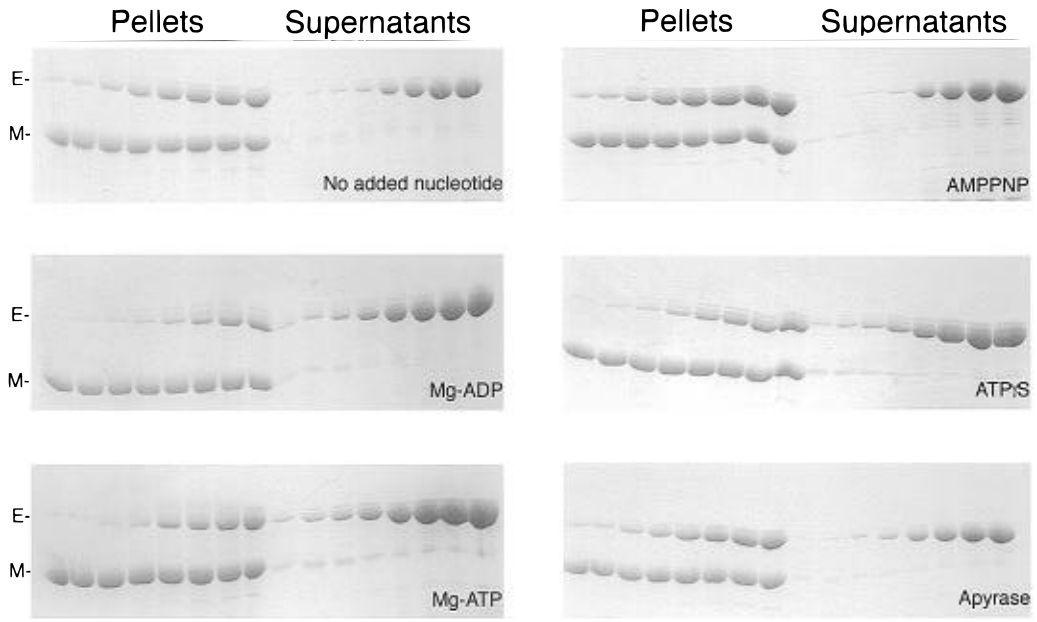

FIGURE 4: Greyscale images of Coomassie-stained SDS-gels from MT pelleting assays. Increasing concentrations, from left to right, of E437GST (0.25−10 μM) were incubated with MTs (2.5 μM) in the presence of various nucleotides and nucleotide analogues. E, E437GST; M, MTs.

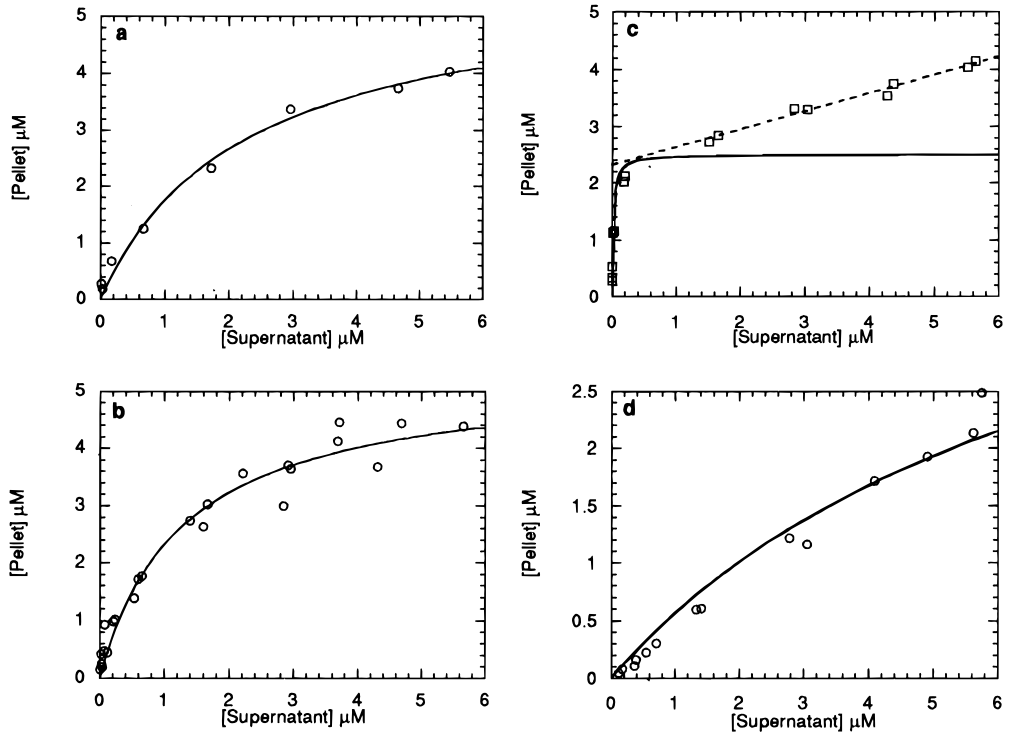

FIGURE 5: Binding isotherms for E437GST (0.25−10 μM) to MTs (2.5 μM) in (a) no added nucleotide, (b) apyrase, (c) AMPPNP, and (d) ATPγS. Motor and MT concentrations are expressed per E437GST motor domain and per tubulin heterodimer. Dissociation constants and binding stoichiometries were estimated by fitting the data to rectangular hyperbolae (solid lines) and are reported in Table 2. Note that the fit for ATPγS is forced to a binding stoichiometry of 2. The AMPPNP data are shown fitted to a stoichiometry of 1 with the dashed line indicating possible weaker nonspecific binding of the motor to the MTs.

95% of the motor pelleting with the MTs. The binding of the motor was again very tight, and we estimate a K_d < 0.1 μM.

The inclusion of either Mg-ATP or Mg-ADP in the assays considerably weakened the binding of the motor to the MTs, and the K_d's under these conditions were estimated to be 1.41 μM and 1.85 μM, respectively (Figure 6). These values are considerably lower than those reported in Table 2, which were estimated to be in excess of 10 μM. The difference is probably a result of the lower ionic strength buffer used in these latter assays. The motor appears to have a slightly higher affinity for MTs in the presence of ATP compared with ADP, again consistent with either the ATP or the ADP·P_i states of the motor binding with higher affinity than the ADP state. The K_d value obtained for the motor in ADP may also be slightly underestimated due to the differing ionic strength contributions from the 5 mM ATP and the 2 mM ADP used in the assays. The maximal binding of the motor in the presence of ATP and ADP was estimated to be 0.94 and 0.89, respectively.

Table 2: Estimated Dissociation Constants and Binding Stoichiometries for E437GST to a Fixed Concentration of Taxol-Stabilized MTs[a]

	Mg-ATP	ATPγS	AMPPNP	Mg-ADP	apyrase	no added nucleotide
K_d (μM)	>10	7.74 (±0.82)*	0.02 (±0.02)†	>10	1.06 (±0.21)	2.22 (±0.10)
stoichiometry	ND	2	1	ND	1.98 (±0.12)	2.36 (±0.10)

[a] The values are derived from the binding isotherms shown in Figure 5. The binding stoichiometries are expressed as the number of E437GST motor domains per tubulin heterodimer. Abbreviations: asterisk, value obtained by forcing the fit to a binding stoichiometry of 2; dagger, value obtained by forcing the fit to a binding stoichiometry of 1 (see text); ND, value not determined.

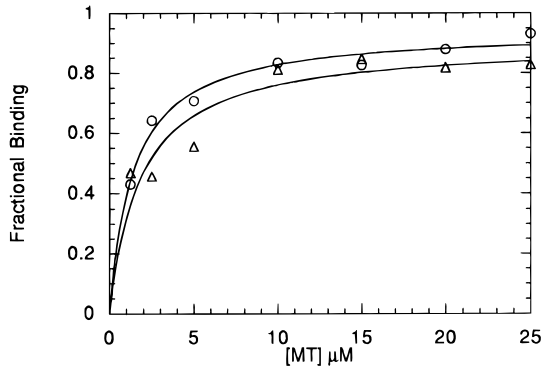

FIGURE 6: Fractional binding of E437GST (1 μM) to MTs (1.25−25 μM) in the presence of (○) 5 mM Mg-ATP and (△) 2 mM Mg-ADP. Values for dissociation constants and the maximal binding of the motor were obtained by fitting the data to rectangular hyperbolae (solid lines). MT concentrations are expressed per tubulin heterodimer.

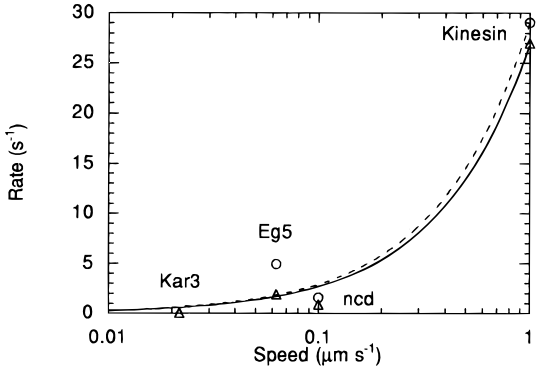

FIGURE 7: Maximal rates of (○) MT-activated mantADP release from Eg5, ncd, and kinesin and (Δ) MT activated ATP turnover by Kar3, Eg5, ncd and kinesin plotted against their respective speeds of MT movement. Linear fits (through the origin) of the mantADP and ATP data are shown as dashed and solid lines, respectively. Kar3 data: Endow et al. (1994). ncd data: Chandra et al. (1993) and Lockhart et al. (1995a). Kinesin data: Cohn et al. (1989) and Lockhart et al. (1995a).

DISCUSSION

Eg5 and kinesin are both plus end directed motors which display a strong sequence homology (~60%) and a high sequence identity (~40%), yet Eg5 moves around 10-fold slower than kinesin. The current data allow us to ask how the kinetic properties of these motors relate to their different rates of physical stepping along MTs. In addition, comparison of the Eg5 data with those of the minus end directed motor ncd should reveal kinetic correlates of reversed directionality. As the speed of movement of these two motors match more closely, the comparison may be more appropriate than that of kinesin and ncd.

E437GST Is a Slow Motor. Eg5 is the first member of the bimC subfamily of MT motors to be kinetically characterized in any detail. The fusion protein E437GST forms stable dimers and is motile, translocating MTs in *in vitro* motility assays at an average velocity of 0.063 μm s^{-1}. Although almost twice as fast as previously reported (Sawin et al., 1992), this velocity is still consistent with Eg5 operating as a slow MT motor relative to either kinesin (~0.60 μm s^{-1}; Cohn et al., 1989) or ncd (~0.10 μm s^{-1}; Chandra et al., 1993). The increase in velocity over that reported previously for Eg5 may be attributed to our relocation of the GST moiety to the C-terminal stalk region of the motor. In the earlier study, the GST was attached to the N-terminus and hence directly to the motor domain of Eg5. The present arrangement may facilitate a more favorable steric interaction between the motor domain of E437GST and the MT. An N-terminal fusion of kinesin and spectrin was also found to move ~2.5 times slower than a C-terminal fusion (Stewart et al., 1993).

Eg5 Is Kinetically Homologous to Kinesin and ncd. In the absence of MTs, mantADP release by Eg5 is so slow that the mantADP is effectively trapped. MT binding specifically accelerates the exchange of mantADP 850-fold, to a maximum rate of 4.94 s^{-1}. Under the same conditions, the overall rate of mantATP turnover by the motor is 1.92 s^{-1}. Eg5 accordingly spends at least 40% of its turnover time in the ADP state, indicating that for Eg5 as for kinesin (Lockhart et al., 1995a; Ma & Taylor, 1995) and ncd (Lockhart et al., 1995a; Shimizu et al., 1995), MT-activated ADP release makes a dominant contribution to limiting the motor's cycle rate.

Again as for kinesin and ncd, the coupling of MT binding by Eg5 to the exchange of active site nucleotide is reciprocal, in that nucleotide species markedly affect the strength of MT binding: ADP stabilizes a weakly MT binding conformation of Eg5, as it does for kinesin and ncd (Ma & Taylor, 1995a; Shimizu et al., 1995; Crevel et al., 1996). ATPγS, a slowly-hydrolyzed analogue of ATP, and AMPPNP, a nonhydrolyzable analogue, tighten the binding. Once more, ncd and kinesin behave similarly, consistent with stronger binding by the ATP and/or ADP·P_i states of all three motors (Hackney, 1994; Crevel et al., 1996). In addition, for all three motors, the nucleotide-free state following ADP release also has a high affinity for MTs (Lockhart & Cross, 1994; Ma & Taylor, 1995a; Crevel et al., 1996).

A Superfamily-Wide Mechanism? Eg5, kinesin, and ncd thus share the same chemically rate-limiting step, MT-activated ADP release, and the same conformational response to nucleotides, at least in regard to their MT binding affinity. The chemical cycle of ATP turnover and the physical stepping of these motors along MTs are coupled, so that the rate limiting chemical step will also set the maximum rate of physical stepping. Strikingly, the speeds of movement of Eg5, kinesin, ncd, and Kar3 [a recently characterized minus end directed motor (Endow (1994)] scale linearly both with their MT-activated ATPase rates and, where measured, with their MT-activated ADP release rates (Figure 7). This result is at least consistent with a uniform coupling efficiency,

in which a general, superfamily-wide physical step consumes a fixed number (perhaps one) of ATP molecules.

MT-activated ADP release switches Eg5 from weak to strong MT binding, as it does for ncd and kinesin. Recent electron microscopy experiments on kinesin suggest that this kinetic step corresponds to a physical tilting of the MT-attached motor domain, consistent with MT-activated ADP release generating force (Hirose et al., 1995). Our data indicate that ADP release is rate-limiting for Eg5, ncd, and kinesin, and raise the possibility of a common, superfamily-wide force-generating conformational change. A definitive test of whether ADP release is force-generating will now require that we measure the influence of physical tension on this rate constant.

ACKNOWLEDGMENT

We thank Dr. Tim Mitchison for suggesting that Eg5 might be kinetically interesting, Dr. Ken Sawin for the Eg5K2 clone, Dr. Isabelle Crevel for performing the *in vitro* motility assays and the BBSRC for funding the Hi-Tech stopped flow spectrofluorimeter.

REFERENCES

Block, S. M. (1995) *Trends Cell Biol. 5*, 169−175.
Chandra, R., Salmon, E. D., Erickson, H. P., Lockhart, A., & Endow, S. A. (1993) *J. Biol. Chem. 268*, 9005−9013.
Cohn, S. A., Ingold, A. L., & Scholey, J. M. (1989) *J. Biol. Chem. 264*, 4290−4297.
Crevel, I. M.-T. C., Lockhart, A., & Cross, R. A. (1996) *J. Mol. Biol.* (in press).
Endow, S. A., Kang, S. J., Satterwhite, L. L., Rose, M. D., Skeen, V. P., & Salmon, E. D. (1994) *EMBO J. 13*, 2708−2713.
Friefelder, D. M. (1982) in *Physical Biochemistry: Applications to Physical Biochemistry and Molecular Biology*, pp 396−401, W. H. Freeman and Co., New York.
Gilbert, S. P., & Johnston, K. A. (1993) *Biochemistry 32*, 4677−4684.
Gilbert, S. P., & Johnston, K. A. (1994) *Biochemistry 33*, 1951−1960.
Gilbert, S. P., Webb, M. R., Brune M., & Johnson, K. A. (1995) *Nature 373*, 671−676.
Goodson, H. V., Kang, S. J., & Endow, S. A. (1994) *J. Cell Sci. 107*, 1875−1884.
Hackney, D. D. (1988) *Proc. Natl. Acad. Sci. U.S.A. 85*, 6314−6318.
Hackney, D. D. (1992) in *Nucleotide triphosphates in energy transduction, cellular regulation & information transfer in biological systems* (Eccelston, J. F., Gutfreund, H., Trentham, D. R., & Webb, M. R., Eds.) pp 13−18, Portland Press, London.
Hackney, D. D. (1995) *Nature 377*, 448−449.
Harrison, B. C., Marchese, R. S., Gilbert, S. P., Cheng, N., Steven, A. C., & Johnson, K. A. (1993) *Nature 362*, 73−75.
Heck, M. M. S., Pereira, A., Pesaento, P., Yannoni, Y., Spradling, A. C., & Goldstein, L. S. B. (1993) *J. Cell Biol. 123*, 665−679.
Hiratsuka, T. (1983) *Biochim. Biophys. Acta 742*, 496−508.
Hirose, K., Lockhart, A., Cross, R. A., & Amos, L. A. (1995) *Nature 376*, 277−279.
Huang, T. G., Suhan, J., & Hackney, D. D. (1994) *J. Biol. Chem. 269*, 16502−16507.
Itaya, K., & Ui, M. (1966) *Clin. Chim. Acta 14*, 361−366.
Laemmli, U.K. (1970) *Nature 227*, 680−685.
LeGuellec, K., Paris, J., Couturier, A., Roghi, C., & Philippe, M. (1991) *Mol. Cell. Biol. 11*, 3395−3398.
Lockhart, A., & Cross, R. A. (1994) *EMBO J. 13*, 751−757.
Lockhart, A., Cross, R. A., & McKillop, D. F. A. (1995a) *FEBS Lett. 368*, 531−535.
Lockhart, A., Crevel, I. M.-T. C., & Cross, R. A. (1995b) *J. Mol. Biol. 249*, 763−771.
Ma, Y. Z., & Taylor, E. W. (1995a) *Biochemistry 34*, 13242−13251.
Ma, Y. Z., & Taylor, E. W. (1995b) *Biochemistry 34*, 13233−13241.
Sawin, K. E., & Mitchison, T. J. (1995) *Proc. Natl. Acad. Sci. U.S.A. 92*, 4289−4293.
Sawin, K. E., LeGuellec, K., Philippe, M., & Mitchison, T. J. (1992) *Nature 359*, 540−543.
Shimizu, T., Sablin, E., Vale, R. D., Fletterick, R., Pechatnikova, E., & Taylor, E. W. (1995) *Biochemistry*, *34*, 13259−13266.
Stewart, R. J., Thaler, J. P., & Goldstein, L. S. (1993) *Proc. Natl. Acad. Sci. U.S.A. 90*, 5209−5213.
Vale, R. D., Schnapp, B. J., Mitchison, T., Steuer, E., Reese, T. S., & Sheetz, M. P. (1985) *Cell 43*, 623−632.
Walker, R. A., Salmon, E. D., & Endow, S. A. (1990) *Nature 347*, 780−782.

BI952318N